Substrate-Induced Conformational Changes of the Perplasmic N-Terminus of an Outer-Membrane Transporter by Site-Directed Spin Labeling†

Gail E. Fanucci,‡ Kelly A. Coggshall,‡ Nathalie Cadieux,§ Miyeon Kim,‡ Robert J. Kadner,§ and David S. Cafiso*,‡

Department of Chemistry and Biophysics Program, and Department of Microbiology, University of Virginia, Charlottesville, Virginia 22904

Received November 6, 2002; Revised Manuscript Received December 16, 2002

ABSTRACT: The structure and dynamics of the N-terminal and core regions of BtuB, an outer membrane vitamin B_{12} transporter from *Escherichia coli*, were investigated by site-directed spin labeling. Cysteine mutants were generated by site-directed mutagenesis to place spin labels in the N-terminal region (residues 1−17), the core region (residues 25−30), and double labels into the Ton box (residues 6−12). BtuB mutants were expressed, spin labeled, purified, and reconstituted into phosphatidylcholine. In the presence of substrate (vitamin B_{12}), EPR spectroscopy demonstrates that there is a conformational change in the Ton box similar to that seen previously for BtuB in intact outer membranes. The Ton box is positioned within the β-barrel of BtuB in the absence of substrate (docked configuration) but becomes unfolded and increases its aqueous exposure upon substrate binding (undocked configuration). This conformational change and the similarity in the EPR spectra between reconstituted and native membranes indicate that BtuB is correctly folded and functional in the reconstituted system. The protein segment on the N-terminal side of the Ton box is highly mobile, and it becomes more mobile in the presence of substrate. Side chains in the region C-terminal to the Ton box also show increases in mobility with substrate addition, but position 16 appears to define a hinge point for this conformation change. EPR line shapes and relaxation data indicate that residues 25−30 form a β-strand structure, which is analogous to the first β-strand in the cores of the homologous iron transporters. When substrate binds to BtuB, this first β-strand remains folded. The EPR spectra of double-nitroxide labels within the Ton box are broadened because of dipolar and collisional exchange interactions. The broadening pattern indicates that the Ton box is not helical but is in an extended or β-strand structure.

The outer membrane of Gram-negative bacteria contains a family of active transport proteins that bind essential nutrients from the external medium and concentrate them in the periplasmic space. In *Escherichia coli* these include FepA, FhuA, and BtuB, which transport iron complexes and vitamin B_{12}, respectively (*1*−*4*). Transport in these proteins is thought to function by a common mechanism (*5*), regardless of the substrate identity. These outer membrane transporters are termed TonB-dependent because they bind to the transperiplasmic protein TonB and derive energy for transport from the inner membrane proton motive force (*2*, *6*). TonB is a transperiplasmic protein that is anchored to the inner cytoplasmic membrane and is associated with the inner membrane proteins ExbB and ExbD. It is thought that an energetically charged conformation of TonB physically interacts with the outer membrane transporters following substrate binding and induces structural changes that lead to the subsequent release of substrate into the periplasmic space.

High-resolution structural models for several outer membrane transporters have been obtained, and these structures all have two distinct domains: a barrel formed from 22 antiparallel β-strands and an N-terminal globular core (Figure 1) (*7*−*10*). The substrate-binding region is located in the large loops that extend above the membrane on the extracellular surface. These loop regions vary in size among the different transporters, presumably because they are adapted to bind different substrates. TonB-dependent transporters all possess a highly conserved sequence near their N-termini, termed the Ton box[1], which is believed to function in coupling the transporter to TonB (*11*), and conformational changes have been observed in the N-terminus of these transporters upon substrate binding. Although the Ton box region is not resolved in the substrate-bound FhuA crystal structure, the first helix (H1), which is C-terminal to the Ton box, is unfolded in the presence of substrate (Figure 1A,B) (*9*). Site-directed spin labeling (SDSL)[2] directed at BtuB in intact outer membrane preparations indicates that the Ton box segment is docked within the barrel of the transporter in the absence of substrate and unfolds upon substrate addition (*12*)[3]. Evidence for this conformational change in BtuB has also been observed through cysteine cross-linking studies

† This work was supported by NIH Grants GM35215 to D.S.C., GM19078 to R.J.K., and NIH NRSA postdoctoral fellowship GM20298 to G.E.F.

* Correspondence should be addressed to the following author. E-mail: cafiso@virginia.edu.

§ Department of Microbiology.

‡ Department of Chemistry and Biophysics Program.

[1] In general, the Ton box motif can be described by A T X X V X Ala, where A is any acidic amino acid, and X is a hydrophobic residue.

10.1021/bi027120z CCC: $25.00
Published on Web 01/24/2003

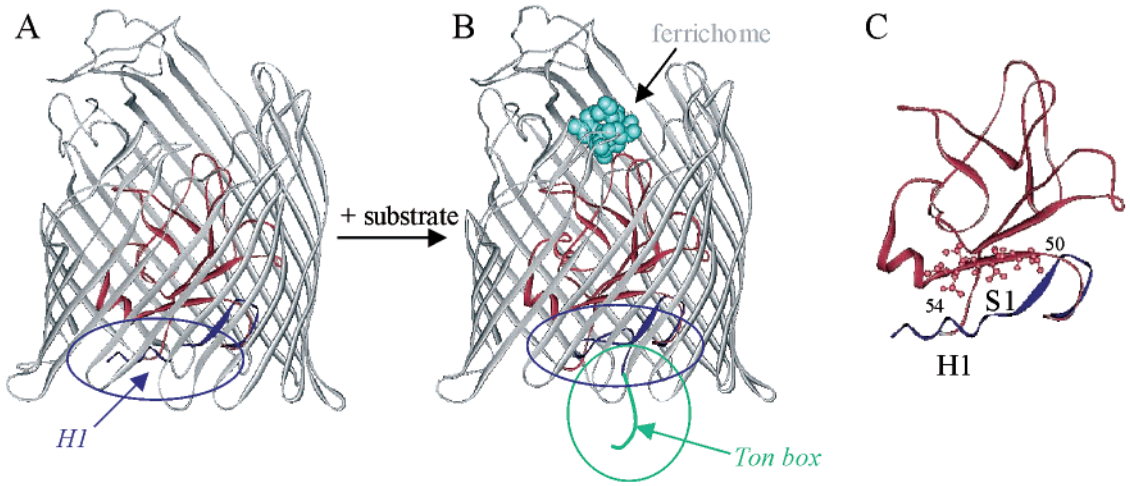

FIGURE 1: Crystal structure of FhuA as viewed from the side of the barrel (A) PDB ID: 1BY3, without substrate showing the H1 helix and (B) PDB ID: 1BY5, with substrate, ferrichrome (cyan), showing that the H1 region has become unfolded and that the Ton box is in an extended conformation. The Ton box region in light green color was artistically drawn and is not part of the original crystal structure. (C) The core region of FhuA showing the H1 helix and the S1 β-strand with residues 50−54 shown in ball-and-stick format. In each structure, the β-barrel is colored in light gray, residues 18−42 are colored in blue with the remaining core region (42−161) colored in light orange.

carried out in intact cells (*13*, *14*). This conformational change likely represents an early step in the transport process, and it may provide a signal to the TonB complex that the receptor is loaded with substrate. The subsequent events in this transport process, including how TonB interacts with the transporter and how substrate is passed through the protein, remain unclear. These events may involve a rearrangement or unfolding of the core of the transporter to produce a channel through which substrate may diffuse (*14*−*16*).

Currently, there is limited information regarding the structure and substrate-induced structural changes that occur in the Ton box. The high-resolution structures of three TonB-dependent iron transporters show the Ton box in either an unresolved or in an extended conformation (*7*−*10*). Furthermore, the substrate-induced structural change of the Ton box, which has been observed in outer membrane preparations by SDSL and EPR, is not observed in these crystal structures. In the present work, SDSL is used to provide additional information on the dynamics, structure, and substrate-induced conformational changes of the Ton box and N-terminal segment of BtuB. SDSL and EPR are carried out on reconstituted purified protein, which allows the labeling of sites that were inefficiently labeled in isolated outer membranes. The work presented here demonstrates that the substrate-induced structural change previously observed for the Ton box in intact outer membranes also occurs in purified protein that is reconstituted into palmitoyloleoylphosphatidylcholine (POPC) bilayers. In the absence of substrate, the Ton box does not adopt a helical structure but appears to be disordered or a β-strand. Substrate-induced structural changes are also observed for labels on either side of the Ton box, and these changes indicate that residues near position 16 form a hinge or pivot region for the conformational change. EPR line shapes and accessibility data are also obtained from SDSL for positions 25−30. These data indicate that this region of BtuB forms the first β-strand in the core of BtuB, homologous with the first β-strands (S1) seen in FepA or FhuA, and that this region remains folded upon the addition of substrate.

EXPERIMENTAL PROCEDURES

Materials

The sulfhydryl reactive methanethiosulfonate spin label (MTSL), (1-oxy-3-methanesulfonylthiomethyl-2,2,5,6-tetramethyl-2,5-dihydro-1H pyrroline) (*17*) was purchased from Toronto Research Chemicals (Ontario, Canada). A diamagnetic analogue of the MTSL spin label was synthesized as described previously (*18*). Nickel (II) acetylacetonate hydrate (NiAA) was obtained from Aldrich Chemical Co. (Milwaukee, WI) and cyanocobalamin (CNCbl) was obtained from Sigma (St. Louis, MO). Octylglucoside (Anagrade) was purchased from Anatrace (Maumee, OH), and 1-palmitoyl-2-oleoyl-*sn*-glycero-3-phosphocholine was purchased from Avanti Polar Lipids (Alabaster, AL).

Methods

Mutagenesis and Isolation of Intact Outer Membranes. A two-step PCR based site-directed mutagenesis technique that has been described previously was used produce cysteine mutants in BtuB (*13*). The mutants were expressed in *E. coli* in strain RK5016 (*metE*), which is a derivative of strain MC4100 [Δ(*argF*−*lac*)*U*169 *araD*139 *rpsL*150 *relA*1 *flbB*5301 *deoC*1 *ptsF*25 *rbsR*22 *non*-9 *gyrA*219] having the additional mutations *metE*70 *argH btuB recA* and which requires vitamin B_{12} to synthesize methionine. To test for

[2] Abbreviations: CNCbl, cyanocobalamin; DM, decylmaltoside; DPPH, α,α′-diphenyl-β-picryl hydrazyl; EPR, electron paramagnetic resonance; HEPES, *N*-2-hydroxyethylpiperazine-*N*′-2-ethanesulfonic acid; MTSL, *S*-(1-oxy-2,2,5,6-tetramethylpyrroline-3-methyl) methanethiosulfonate; NiAA, nickel (II) acetylacetonate; OG, octylglucoside; PCR, polymerase chain reaction; OM, outer membrane; SDSL, site-directed spin labeling; POPC, 1-palmitoyl-2-oleoyl-*sn*-glycero-3-phosphocholine.

[3] The substrate-bound form of the Ton box is referred to as either an unfolded or an undocked form, and these terms are used here interchangeably. The EPR spectra for the substrate-bound form of the Ton box are consistent with those expected for an unfolded or extended protein strand. The termed undocked attaches a functional significance to this unfolding. In its undocked or unfolded form, the Ton box facilitates interactions between BtuB and Ton B.

Scheme 1

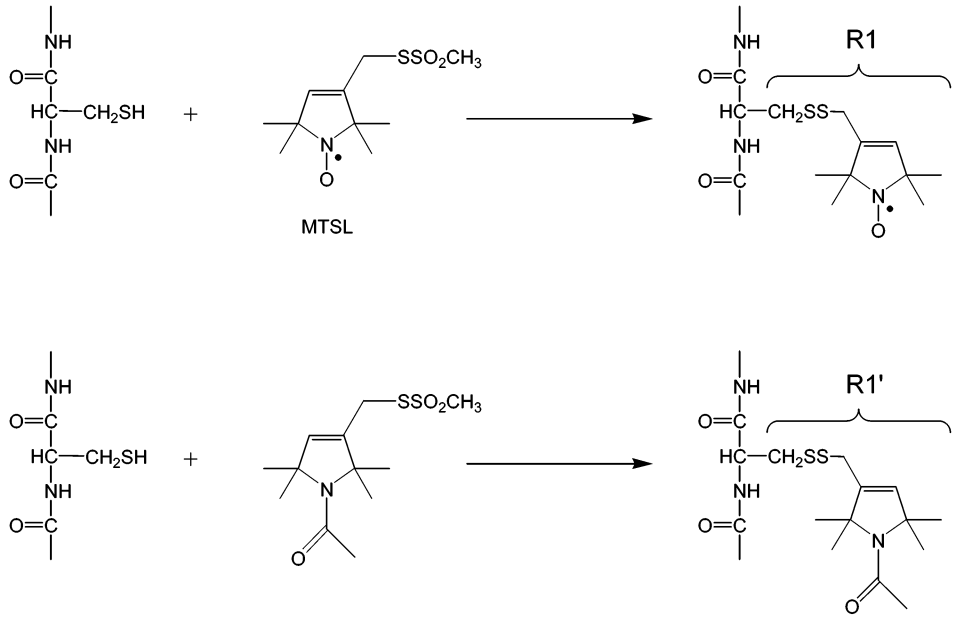

functionality, the different mutants were grown on minimal A salt agar supplemented with 0.02% glucose, 0.01% Arg, and various concentrations of vitamin B_{12} (0.1−5000 nM) in place of methionine. The comparison was made with growth on similar plates containing 0.01% Met, as previously described (*19*). All the BtuB Cys mutants were therefore tested for their ability to use vitamin B_{12} in place of methionine for growth. They were all found to function as well as the wild-type protein in this growth assay. Outer membranes were grown and isolated as described previously (*15*).

Protein Purification and Spin Labeling. Outer membrane fractions were solubilized by octylglucoside (OG), and all single- and double-labeled MTSL (R1) BtuB mutants were labeled and purified by anion exchange chromatography as described previously (see Scheme 1) (*20*). The purity of samples was determined by SDS−PAGE electrophoresis. Silver staining revealed that lipopolysaccharides were present in the purified BtuB fractions, but concentrations were not determined. For labeling with R1 and the diamagnetic R1′, molar ratios of 30:70 were added to the solubilized membrane supernatant and allowed to react for 4 h before purification by the same FPLC procedure used for the R1 mutants.

Liposome Reconstitution and Sample Preparation. Purified protein samples were reconstituted into POPC vesicles in HEPES buffer by the dialysis of OG from mixed POPC/OG micelles as described previously (*20*). For measurements with vitamin B_{12} (CNCbl), 5 μL of sample was mixed with 1 μL of a vitamin B_{12} stock solution to give a final B_{12} concentration of 450 μM. For the power saturation experiments, 4.7 μL of sample and 1.3 μL of 100 mM NiAA were mixed to produce a 20 mM NiAA solution. In both cases, multiple freeze thaw cycles were performed to ensure that the added reagents had equal distributions inside and outside the vesicles.

Electron Paramagnetic Resonance. EPR spectroscopy was performed on a Varian E-line 102 series X-band spectrometer equipped with a loop−gap resonator (Medical Advances, Milwaukee, WI). Labview software, which was generously provided by Drs. Christian Altenbach and Wayne Hubbell (UCLA), was used for digital collection and analysis of data. All spectra for line shape analyses were recorded at 2.0 mW incident power with a modulation amplitude of 1.0 G, and these samples were prepared in glass capillary tubes with a 0.8 mm i.d. (VitroCom, Mountain Lakes, NJ). For power saturation measurements, the samples were placed in gas-permeable TPX tubes (Medical Advances, Milwaukee, WI), and spectral amplitudes were measured using microwave powers that varied from 0.25 to 100 mW. During these experiments, either a stream of air (oxygen accessibility) or nitrogen (baseline measurement and metal relaxing agent) was used to purge the samples. The $P_{1/2}$ values, which are related to the product $(T_{1e}T_{2e})^{-1}$, were then determined from the power saturation curves as described elsewhere (*21*). These values were then normalized against the $P_{1/2}$ value for DPPH and used in turn to determine the collision parameter Π for each reagent. The parameter Π is related to the change in T_{1e} of the nitroxide by the frequency with which either NiAA or O_2 collide with the R_1 side chain (*22*).

EPR spectra of double mutants were acquired at room temperature and at −130 °C by passing cooled nitrogen gas over the sample and loop−gap resonator. Spectra at −130 °C were acquired with an incident microwave power of 20 μW, whereas those at room temperature were acquired with 2 mW. Estimates of distances were determined from dipolar broadened spectra of double-labeled mutants at −130 °C by taking a ratio of spectral amplitudes (d_1/d_0) and comparing the values to those obtained for the potassium channel KcsA as described previously (*18*). Distances were also determined as described previously by finding the Pake broadening function, which when convolved with the noninteracting spectrum (in the case the sum of the single-labeled spectra) reproduced the experimental spectrum (*23*).

RESULTS

Ton Box in Reconstituted BtuB Undergoes a Docked to Undocked Transition in the Presence of Substrate. Previous

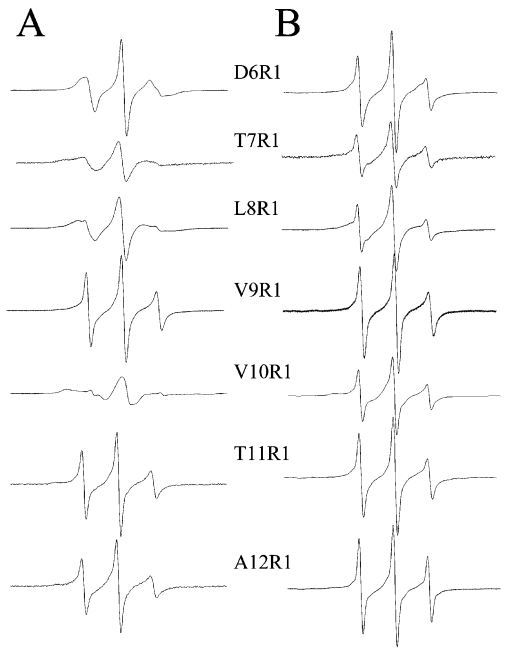

FIGURE 2: EPR spectra normalized to equal areas for Ton box mutants labeled with R1. (A) Samples reconstituted into POPC vesicles. (B) Samples reconstituted into POPC vesicles with 450 μM vitamin B_{12}. Spectra are plotted with equal scaling in the *y* dimension, and each spectrum was acquired with a 100 G sweep width.

SDSL of the Ton box region of BtuB was performed in isolated outer membrane fragments from *E. coli*. These experiments demonstrated that the conformation of the Ton box is docked within the BtuB barrel in the absence of substrate, and it unfolds upon substrate (vitamin B_{12} or CNCbl) binding (*12*). Shown in Figure 2A are the EPR spectra for the single spin-labeled BtuB mutants in the absence of substrate, which have been labeled, purified, and reconstituted into POPC bilayers as described above (see Methods). The EPR line shapes indicate that a wide range of motion is present for the labeled side chains within the Ton box region[4]. For example, the EPR spectra for positions 7 and 10 are broad, indicating that the R1 side chain is in tertiary contact, whereas the relatively narrow spectra at positions 9, 11, and 12 indicate that R1 is highly mobile at these sites. Collectively, the EPR line shapes for the reconstituted samples are similar to those observed for BtuB in the isolated outer membrane fragments. For the reconstituted system, substrate addition (Figure 2B) results in a loss of the tertiary contacts present in the closed state, indicating that a conformational change has taken place. In the presence of substrate, the EPR line shapes for residues 6−8 and 10 are now similar to those for residues 9, 11, and 12. These changes were also seen in our earlier studies of BtuB labeled in the outer membrane, and the spectra shown in Figure 2 indicate that the transition from a docked to undocked configuration of the Ton box also occurs for BtuB in the reconstituted system.

[4] In general, the mobility of the nitroxide side chain is indicted by the breadth of the EPR spectrum. Broader features are present in the EPR line shapes for side chains with lower mobility. The term mobility refers to both the rate and the amplitude of motion of the R1 side chain, and we make no attempt to separate the contributions of these two factors in line shapes. The spectra presented here are also normalized against their second integrals so that the EPR amplitudes are a function of the label mobility.

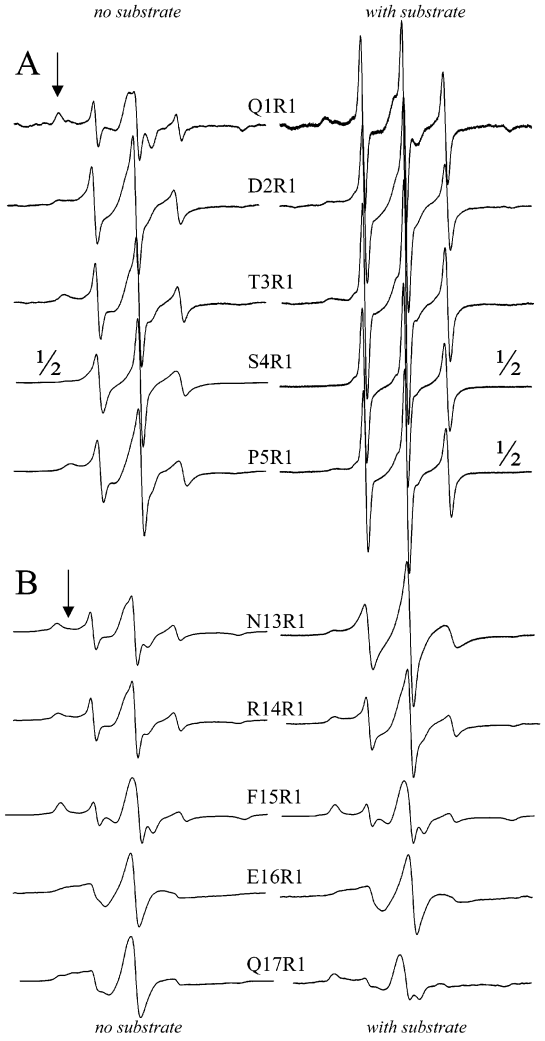

FIGURE 3: EPR spectra normalized to equal areas for the extended Ton box mutants labeled with R1 without and with substrate. (A) N-terminal R1-labeled BtuB mutants and (B) C-terminal R1-labeled BtuB mutants reconstituted into POPC vesicles. In each case, the right-hand columns show the EPR spectra acquired in the presence of substrate, vitamin B_{12}. Spectra are plotted with equal scaling in the *x* dimension, and each spectrum was acquired with a 100 G sweep width. The arrows in the figure show the underlying broad components.

EPR Line Shapes for Residues on Either Side of the Ton Box Regions in Both Docked and Undocked States Indicate a Hinge Point for the Conformational Change. The spin-labeled side chain R1 was incorporated into positions on both the N- and the C-terminal sides of the Ton box. Figure 3A shows EPR spectra normalized for equal areas for residues 1−5, N-terminal to the Ton box, with the right column representing the substrate-bound state. In the absence of substrate, the EPR line shapes for residues 1−5 are very narrow, indicating that this segment has a high degree of motion. In a few of these spectra, an underlying broad component can be observed (arrows, Figure 3). This broad component represents a population of R1 side chains that are restricted in their motion. Except for positions 1 and 5, this component represents a minor fraction of the total R1 population. The presence of two different line shapes can

result from a variety of factors that include multiple conformations of the side chain or peptide backbone.

When substrate is added, the amplitudes of each of the spectra for residues 1−5 increase. Both a further narrowing of the line widths and a reduction in the relative percentage of the broader component causes an increase in normalized amplitudes for these already highly motionally averaged spectra. The increased motion of this segment is consistent with the change seen in the Ton box, which converts from a docked to an undocked configuration in the presence of substrate. The high degree of motional averaging observed in both the docked and the undocked states indicates that the N-terminal segment is not in tertiary contact or folded into the barrel in either state. Thus, we can infer that this region of the protein is highly dynamic and unstructured. The broader component may represent a minor conformation of the N-terminal segment where the side chains contact the barrel or other parts of the protein and rapidly interconvert with the more mobile conformation.

Shown in Figure 3B are the EPR spectra normalized to equal areas for sites C-terminal to the Ton box (residues 13−17). It is immediately apparent that the spectra for R1 at sites 13−17 are broader than those for R1 at sites 1−5, indicating that the R1 side chain at sites C-terminal to the Ton box are less mobile than the N-terminal sites. The line shapes for residues 13−17 are representative of spectra for the R1 side chains that are in tertiary contact (*24*). For positions 13−15, two components can be observed in each spectrum. These features may represent either two conformations for the labeled side chain or two backbone configurations. Only a single spectral component is present in the EPR spectra of R1 at sites 16 and 17. When substrate is added, the spectrum for position 13 changes, but the spectrum for the liganded state is much broader than that detected for sites within the Ton box. Additionally, the line shapes for sites 13−17 in the substrate-bound form are broader than those for sites 6−12 in the undocked form of the Ton box (Figure 2B). Interestingly, the addition of substrate does not significantly change the EPR spectrum of R1 at sites 14−16. Furthermore, addition of substrate for site 17 results in an EPR line shape that is broader than observed for the unliganded state. These results indicate that there is little change in mobility for sites 14−16 with site 17 becoming less mobile when substrate binds. The pattern of line shapes from the Ton box through to position 17 suggests that positions 15−17 form part of a hinge region for the undocking of the Ton box.

Figure 4A is a plot of the change in normalized intensities ($I_{NB12} - I_N$) for all of R1-labeled sites in the presence (I_{NB12}) and absence (I_N) of substrate. For residues 1−13, the positive values indicate that these sites become more mobile when substrate is bound. Sites 14 and 15 become only slightly more mobile, and in contrast, site 17 becomes more immobilized. This figure clearly shows the changes in the R1 label dynamics between the docked and the undocked states. Figure 4B plots the scaled mobilities, M_s, for each of the EPR line shapes for residues 1−17 in the undocked substrate-bound conformation. The scaled mobility, M_s, is a parameter that can be used to compare the relative mobility of R1-labeled side chains (*25*, *26*). Remarkably, the values span a range from those that are close to the most mobile sites seen for R1 in proteins ($M_s = 1$) to a value that is one of the least

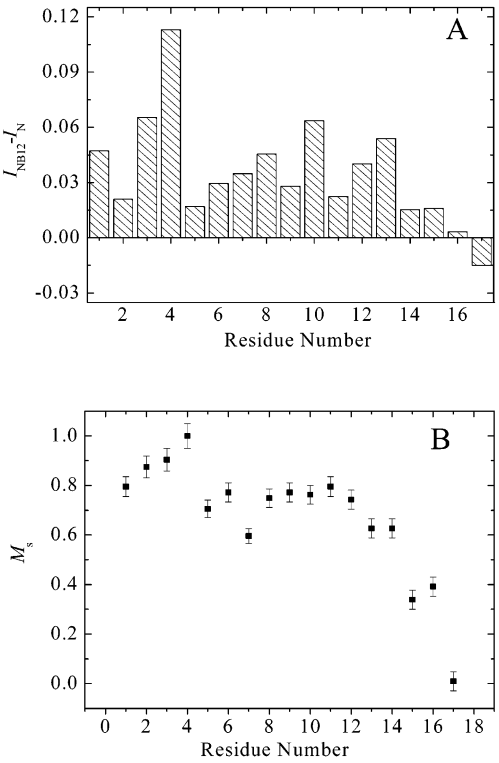

FIGURE 4: (A) Plot of the change in normalized intensity, $I_{NB12} - I_N$, of the central first-derivative resonance of the EPR spectra for sites 1−17 in the absence, I_N, and presence, I_{NB12}, of substrate. Error bars are not displayed because the error for each normalization procedure was at maximum 3% of the values. (B) Plot of the scaled mobility, M_s, for sites 1−17 in the presence of substrate.

mobile ($M_s = 0$)[5]. The pattern of scaled mobilities plotted in Figure 4B suggests that this segment is tethered at one end but has a high degree of motion at the N-terminal end, and the pattern suggests (as mentioned above) that residues 16 and 17 are near a hinge point for the substrate-induced conformational change.

Ton Box Does Not Have a Helical Structure and Is Highly Mobile. As discussed elsewhere, the *i*, $i + n$ pattern of tertiary contact observed for the EPR spectra of residues 6−12 in the Ton box segment in its closed configuration is roughly consistent with that expected for a helix (*12*). However, the EPR spectra for R1 at positions 9, 11, and 12 are not typical of those obtained for the R1 side chain incorporated into a well-formed helix (*24*). The EPR line shapes for R1 at positions 9, 11, and 12 result from a high degree of motional averaging. These line shapes correspond to a spin label with a correlation time of about 1 ns or less and have narrower spectral features than previously seen for the R1 side chain when located at exposed sites on flexible helices (*27*). To determine whether the structure of the Ton box is a

[5] The scaled mobility, M_s, is a parameter that can be used to compare the relative mobility of R1-labeled side chains. This parameter is defined as $M_s = (\delta^{-1} - \delta_i^{-1})/(\delta_m^{-1} - \delta_i^{-1})$, where δ is the central nitroxide line width, and δ_m and δ_i represent the line widths of the most mobile and immobile protein associated R1 labels observed. Here, these values were taken as 8.5 and 1.8 G, respectively. These limiting values were determined from spectra reported here and in earlier work (see ref *26*). Values of M_s were determined only for spectra having a single motional component since the value of M_s, in the case where both broad and narrow components are present, would only reflect the mobility of the narrower component. Here it is only calculated for the EPR spectra of the undocked substrate-bound state.

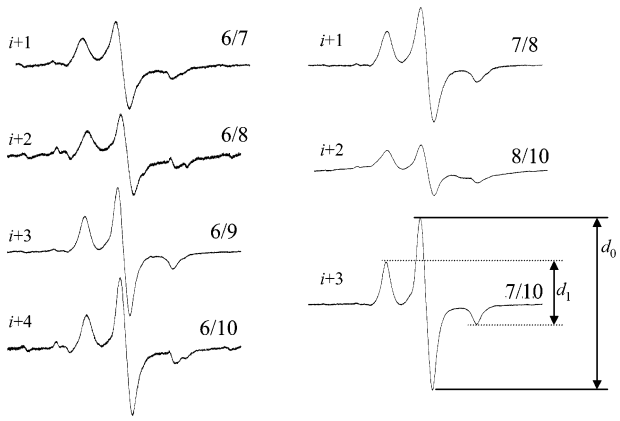

FIGURE 5: EPR spectra of each of the rigid limit double-labeled R1 Ton box mutants. Spectra were acquired at −130 °C at 2 μW incident microwave power. For easy comparison of the degree of line broadening, the spectra are normalized to equal areas and are plotted on the same *y* scale. Each spectrum was acquired with a 200 G field scan. The d_1/d_0 ratio is defined as the height of the high and low field transitions over the height of the center field transition and is shown graphically for mutant 7/10. Spectra for mutants 6/8 and 6/10 have some baseline distortions that result from contaminants in the glass capillaries.

Table 1: EPR Spectral Parameters for Double-Cys R1 Mutants at Room Temperature and −130 °C

mutant	$i+n$ $n=$	ΔH_{rt} (±0.1 G)	ΔH_{-130C} (±0.2 G)	d_1/d_0[a] (−130 °C) (±0.2)	interaction strength	approx. distance[b]
6R1/7R1	1	8.3	11.1	0.47	moderate	13−14
7R1/8R1	1	7.0	11.1	0.45	moderate	15
6R1/8R1	2	4.1	10.9	0.44	moderate	15
8R1/10R1	2	8.0	11.6	0.58	strong	7
6R1/9R1	3	2.7	10.0	0.41	weak	18
7R1/10R1	3	5.4	10.5	0.36	very weak	21
6R1/10R1	4	3.4	10.7	0.35	very weak	21

[a] Typical d_1/d_0 values obtained for single (noninteracting) R1 mutants ranged from 0.36 to 0.40. The distances estimated from the d_1/d_0 ratio appear to be slightly longer in some cases than those estimated using a Fourier convolution approach. This appears to be due to a fraction of single-labeled protein present in the sample. [b] Distances were estimated from d_1/d_0 values presented for KcsA (*18*).

disordered irregular helix or if it has a different configuration, a series of double-Cys mutants with varied *i*, *i* + 1 to *i*, *i* + 4 spacings were prepared and labeled. Figure 5 shows the low-temperature EPR spectra obtained for the double R1-labeled cysteine mutants: 6/7, 6/8, 6/9, 6/10, 7/8, 8/10, and 7/10. The degree of dipolar broadening in this rigid limit is estimated from d_1/d_0, which is the ratio of the intensities of the low field and high field transitions to the intensity of central transition of the first derivative EPR spectrum of the MTSL nitroxide radical (*28*). Values of $d_1/d_0 < 0.4$ indicate that very little dipolar interaction occurs, whereas values >0.45 report interactions of moderate strength. The values of d_1/d_0 for each of the pairs are given in Table 1. The values for the *i*, *i* + 3 and *i*, *i* + 4 pairs are <0.4, indicating weak or no dipole interactions. In contrast, the d_1/d_0 values for the *i*, *i* + 2 and *i*, *i* + 1 pairs range between 0.45 and 0.58, indicating the presence of moderate to strong dipolar interactions. This finding indicates that the Ton box structure in the closed conformation is not α-helical, but it instead has a β-strand or extended conformation.

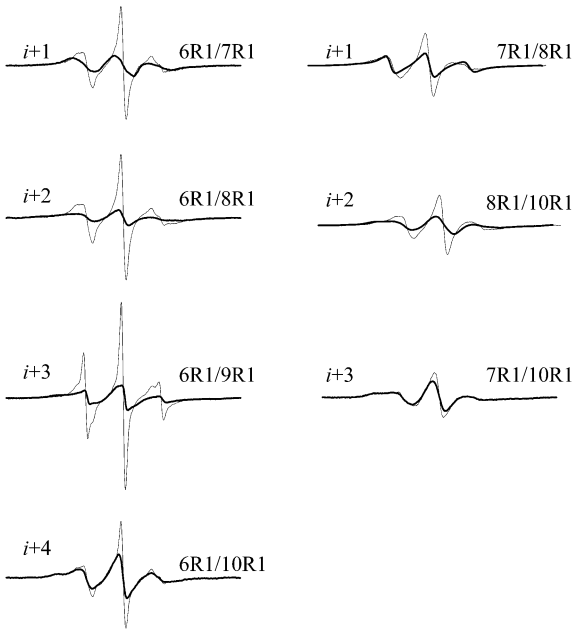

FIGURE 6: Comparison of EPR spectra acquired at 25 °C of the double-labeled R1 Ton box mutants (black thick lines) to each of the corresponding summed noninteracting singles spectra (grey thin lines). Spectra are normalized to equal areas and plotted with the same *y* scaling for easy comparison. All spectra were acquired with a 100 G field scan.

Figure 6 shows the room temperature EPR spectra normalized to equal areas of each of the double R1-labeled mutants (thick lines) overlain upon the summed spectra of the noninteracting singles. In each case, except 6R1/10R1 and 7R1/10R1, the EPR spectra of the double-labeled mutants are broader and have lower amplitudes than the spectra of the corresponding noninteracting pairs. The EPR spectra of this series of double R1-labeled mutants exhibit a much greater degree of line broadening at room temperature than expected from the relative strengths of the dipolar interactions observed in frozen samples. A reasonable interpretation of the additional broadening is that there is a significant degree of motion in the backbone or side chains at room temperature, resulting in collisions between labels resulting in Heisenberg exchange. In all but a few cases, it was not possible to cleanly convolute dipole Pake patterns with the summed noninteracting spectra to reproduce the EPR line shapes of the interacting double-labeled samples. The distances reported in Table 1 are approximate and were determined from the d_1/d_0 ratios as described previously (*18*).

Presence of R1 May Undock the Ton Box When Incorporated at Certain Positions. We were interested in determining whether the presence of the R1 side chain at certain positions might promote the undocked or unfolded configuration of the Ton box because several observations suggested that this could be occurring. As noted above, the EPR line shapes for V9R1, T11R1, and A12R1 in the absence of substrate reflect a high degree of side chain and backbone mobility that is normally expected for an unstructured protein segment. This degree of mobility is surprising because V9R1 and T11R1 flank V10R1, which is the most immobile label in the Ton box. In addition, little or no change is seen for the spectra of R1 at positions 9, 11, or 12 upon substrate addition (Figure 2).

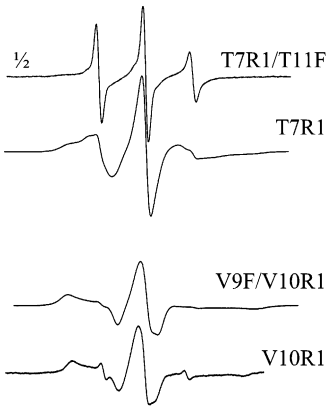

FIGURE 7: EPR spectra comparing the effects of phenylalanine substitutions on the Ton box conformation. Spectra are discussed in the text. All spectra are normalized to equal areas and are plotted with the same *y* scaling except for T7R1/T11F where the *y* axis is doubled in value to make the spectrum fit nicely in the figure. Spectra were acquired with a 100 G field scan.

To determine whether the R1 side chain might perturb the docked structure, we performed two sets of experiments. First, we prepared two double mutants containing both a phenylalanine and a cysteine (for R1 labeling). Phenylalanine is a larger residue, which would mimic insertion of the spin label, and it was substituted at positions 11 and 9. R1 was incorporated at positions 10 and 7, which show contact in the docked state and should report the state of the Ton box. The EPR spectra for V9F/V10R1 and T7R1/T11F reconstituted into POPC are shown in Figure 7 along with the spectra of V10R1 and T7R1. The spectrum for T7R1/T11F is dramatically different than that for T7R1 and is similar to T7R1 in the presence of substrate. This result indicates that the placement of a phenylalanine at residue 11 unfolds the Ton box. On the other hand, the spectrum of V9F/V10R1 is very similar to that of V10R1 indicating that the substitution of phenylalanine at position 9 does not alter the Ton box configuration. This result suggests that a single R1 substitution may spring open the Ton box when substituted at position 11 but that the Ton box may remain folded when R1 is substituted at position 9.

The second set of experiments to address this question involved labeling the double-cysteine mutants V9C/V10C and T7C/T11C with a mixture of MTSL and a nonmagnetic analogue R1′ in a 30:70 R1/R1′ ratio (Scheme 1). These mutants were chosen so that one R1 site (7 or 10) would provide a broad spectrum, with the second site (either 9 or 11) providing a narrow EPR signal. If R1 at positions 9 or 11 undocked the Ton box, then the spectrum of the R1/R1′ double mutant should be the sum of the corresponding single spectra for the substrate-bound (undocked) configuration. However, if these R1 substitutions do not perturb or unfold the Ton box, then the resultant line shapes should resemble the sum of the spectra for the docked state (unlignaded), and the double-labeled spectra should retain some broader features.

Figure 8A,B compares the spectra of the 9/10 and 7/11 R1/R1′ mutants to the summed spectra for the R1-labeled single mutants in the absence of substrate (docked state) and the presence of substrate (undocked state), respectively. In both cases, some double R1 labeling has occurred, which leads to a small amount of dipole broadening. The broad

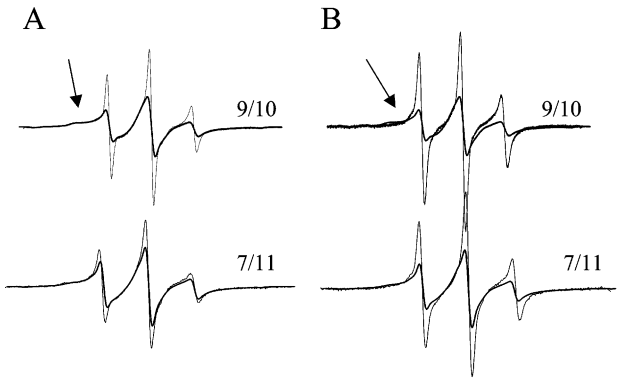

FIGURE 8: EPR spectra comparing double mutants 9/10 and 7/11 that are under labeled with a 30:70 R1/R1′ mixture (thicker lines) to (A) the spectra of each of the appropriate summed singles labeled with R1 (thin lines) in the closed state (no substrate) and to (B) the spectra of each of the appropriate summed singles labeled with R1 (thin lines) in the open state (with vitamin B_{12}). The arrows in the figures show the broad component coming from site 10. The spectra are normalized to equal areas and are plotted on the same *y* scales. Spectra were acquired with a 100 G field scan.

feature in the spectrum of 9/10 R1/R1′ (indicated by arrows in the figure) can be fit only when this spectrum is compared to that of the summed singles for 9R1 and 10R1 in the closed state. However, the spectrum for the 7/11 R1/R1′ is not well-represented by either of the summed single states, thus making it hard to draw a conclusion about the effect of R1 at site 11. From the results of this experiment and the results of the phenylalanine substitution at site 9, we conclude that V9R1 does not perturb the docked conformation of the Ton box. On the other hand, it is likely that T11R1 promotes the undocked configuration of the Ton box. Hence, the relatively narrow line shape (and high mobility) observed for 11R1 (and possibly for 12R1) may be an artifact of the incorporation of the spin label.

Beginning of the β-Strand Structure of the Core Regioncon of BtuB Is Identified by EPR Line Shapes and Relaxation Measurements. Shown in Figure 9 are EPR spectra for R1 at positions 25−30. The solid lines are spectra acquired in the absence of substrate, whereas the dashed lines are spectra collected after substrate addition. It is apparent that the line shapes do not change significantly when vitamin B_{12} is added, indicating that no conformational change occurs in this region of the protein upon substrate binding. Thus, the dramatic unfolding observed for the Ton box is limited to the N-terminal region of the protein core. The pattern of mobility seen for R1 at these sites provides an indication of its secondary structure, and Figure 10A plots the normalized central intensity, I_N, of each of the spectra in Figure 9. The resulting *i*, *i* + 2 periodicity is indicative of a β-strand. In addition, the accessibility parameters, Π, for both oxygen and NiAA (Figure 10B) have an *i*, *i* + 2 pattern also indicating a β structure. A comparison of these Π values to those measured for sites in proteins of known structure (*29*, *30*) indicates that the even numbered residues in this β-strand have partial aqueous exposure, whereas the odd numbered residues are more protected or buried.

DISCUSSION

The work described here was carried out with several objectives in mind. One objective was to determine whether

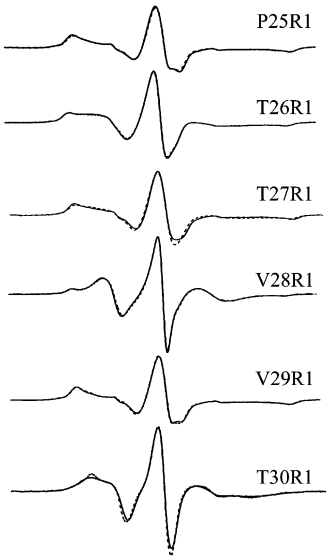

FIGURE 9: EPR spectra for R1-labeled sites in the first β-strand of the core without substrate (solid lines) and in the presence of vitamin B_{12} (dashed lines). The spectra are normalized to equal areas and are plotted with the same *y* scales. Spectra were acquired with a 100 G field scan.

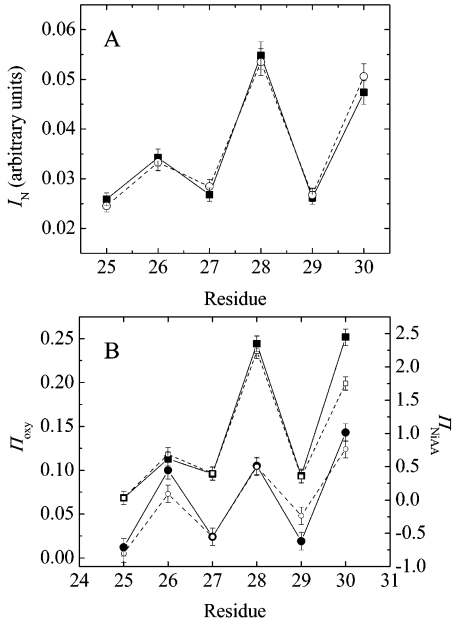

FIGURE 10: (A) Plots of the normalized intensity, I_N, of the central first-derivative resonance of the EPR spectra shown in Figure 9 for sites 25−30 in the absence (■) and presence (○) of substrate. (B) Collision accessibilities (Π) for oxygen (no substrate, ●; with substrate, ○) and NiAA (no substrate, ■; with substrate, □) for residues 25−30 determined using air (20% oxygen) and 20 mM NiAA (with an N_2 purge background), respectively. A β-strand (*i*, $i + 2$) periodicity is clearly revealed in both of these data plots.

the substrate-induced conformational change of the Ton box observed previously in intact outer membrane samples also occurred when BtuB was purified and reconstituted into a defined lipid mixture. Although the Ton box region can be spin labeled while BtuB is in the intact outer membrane (*12*, *15*), reconstitution of the protein is necessary because it was found difficult to reproducibly label other segments of this protein without detergent solubilization. A second objective was to determine those positions on the N- and C-terminal sides of the Ton box that are involved in the substrate-induced conformational change. Third, we wanted to determine whether segments deeper in the core of BtuB also unfolded upon substrate addition. Finally, we were interested in examining the conformation of the Ton box in its closed state.

The data obtained here clearly demonstrate that the Ton box of BtuB is folded in the same manner in the reconstituted system as it is in the native system. Further, the conformational change observed for the Ton box in intact outer membranes when substrate binds also occurs for BtuB reconstituted into POPC vesicles. Retention of the conformational change indicates that BtuB is functional in the reconstituted system. Additionally, previous SDSL and EPR spectroscopy of putative β-barrel segments of BtuB reconstituted into this same lipid system indicate that the BtuB barrel is properly folded (*20*).

The N-terminal side of the Ton box (residues 1−5) is a highly dynamic and disordered segment of the protein. The additional motion that is observed upon substrate binding (Figure 3) reflects an additional loss of conformational constraint that is expected to occur upon the undocking of the Ton box. In the presence of substrate, this segment is one of the most mobile protein segments that has been investigated by SDSL (*26*). The segment on the C-terminal side of the Ton box is more structurally ordered than the N-terminal side, and the EPR spectra indicate that a hinge for the undocking of the Ton box when substrate binds is located near position 16. Residues further in core (positions 25−30) form a β-strand but do not become unfolded upon substrate addition. It should be noted that this β-strand is homologous with segments in FepA and FhuA that form the first β-strand (S1) within the core (*7*, *9*). In FhuA, residues 49−54 form this strand, and in FepA it is formed from residues 27−32. In each case, residues on one face of the strand have a greater exposure to the periplasm than the other face, and the strands are tilted within the core so that one end is more buried. The collision parameters reported here (Figure 10) are consistent with the sidedness of the strand in FepA and FhuA and suggest that the strand is also tilted in BtuB.

The model that can be generated from these data for the substrate-bound form of BtuB places residues 1−15 in an unstructured strand that is free to diffuse toward the periplasm with residues 16 and 17 remaining tethered to the core. As indicated previously (*14*, *15*), the substrate induced unfolding of this N-terminal segment may trigger the interaction with TonB, either by directly recognizing TonB or facilitating an interaction between TonB and BtuB. Disulfide cross-linking indicates that residues within the Ton box directly cross-link with positions in TonB suggesting that there is a direct interaction between the Ton box and TonB (*13*). Although there is limited information from crystallography on substrate-induced changes in the Ton box of TonB-dependent proteins, the structural changes seen previously in FhuA are consistent with the results obtained here. They also indicate that the most significant changes are localized to the N-terminal end of the protein (*9*).

As indicated above, we found that many segments in BtuB are poorly labeled in intact outer membranes. However, efficient labeling can be achieved by solubilization and reconstitution procedures. We believe this occurs because both the dynamics of the protein and its structure are

perturbed in the micelle environment where the MTSL reaction is carried out. In a previous SDSL study on BtuB, the backbone dynamics of the β-barrel region of BtuB were found to be dramatically enhanced in the presence of mixed micelles formed from POPC and OG (*20*). These changes were particularly dramatic near the periplasmic end of the barrel. We have also observed that a portion of the N-terminus of BtuB (including the Ton box) becomes unfolded when placed in OG or DM micelles, and the unfolding is reversed when the protein is reconstituted into a lipid bilayer environment (Fanucci and Cafiso, unpublished). Both increased protein dynamics and partial unfolding likely increase the accessibility of the MTSL to the various mutant cysteine sites.

The sequential pattern of EPR line shapes obtained previously for the Ton box indicated that it might have a helical periodicity (*12*). Here, a series of double-labeled cysteine mutants were labeled, and the degree of dipolar broadening was determined for sites within the Ton box. The degree of dipolar broadening observed in the rigid limit spectra was greatest for pairs of residues having an i, $i + 2$ spacing consistent with the conclusion that the Ton box in its docked state is not helical but may assume a β-strand structure. For the spectra presented here, we attempted to analyze the distances between spin pairs using a Fourier convolution approach (*23*, *31*). For the labeled mutant 7R1/10R1, the analysis yielded a bimodal distance distribution with one distance centered at 12 Å and the other at 18 Å. As discussed elsewhere, these distributions may reflect different orientations for the R1 side chain (*23*), but in any case, the distances are not consistent with an α-helical structure (*31*). The distance profile generated from analysis of the low-temperature spectrum of 7R1/10R1 was used to successfully simulate the room temperature double R1-labeled spectrum of this mutant. However, this type of analysis was not possible for any other labeled pair that we examined. As indicated above, Heisenberg spin exchange appears to give rise to additional line broadening that is not seen at low temperature, and this apparently accounts for our inability to match both low- and room-temperature distance distributions. The presence of Heisenberg exchange suggests that at room temperature there is a significant degree of motion for many of the residues in the Ton box, which leads to collisions between R1 side chains. As a result of these complications, we have not attempted a more detailed analysis of the distances between the other spin pairs.

Previous work has shown that the R1 substitution is no more perturbing than any other single amino acid substitution (*24*). The effects of single R1 substitutions on the folding of T4 lysozyme have been examined and were found to have only a minor effect on the thermal stability of this protein. R1 substitutions in the core region produced the largest effects but still allow the protein to correctly fold. In fact, for these substitutions, the protein was only destabilized by several kcal/mol. In the case of BtuB, the R1 substitution at position 9 does not perturb the Ton box conformation, but the substitution at position 11 (and possibly position 12) may perturb or alter the Ton box conformation from its normal docked state. This finding could account for the relatively mobile line shapes seen at positions 11 and 12 in the absence of substrate, as well as the absence of a substrate-induced line shape change. The likely perturbation by R1 at certain sites in the Ton box and the effects noted above with detergents suggest that the free energy difference between docked and undocked conformations of the Ton box is small. Indeed, careful measurements of the broad (docked) and mobile (undocked) components in the EPR spectra indicate that this difference is on the order of a few kcal/mol (Fanucci and Cafiso, unpublished).

In summary, the data reported here provide information on the structure and mobility of the Ton box segment of BtuB in both its docked and its undocked conformations. The data indicate that the Ton box in the reconstituted system exhibits the same structural change observed in intact outer membranes. In its docked state, the Ton box is in a β-strand or extended conformation rather than a helical configuration. Residues 1 to 15 become undocked from the BtuB core upon the addition of substrate, and positions 16 and 17 appear to be near a hinge responsible for opening the Ton box. Positions 25−30 form a β-strand within the core of BtuB that remains folded in the presence of substrate. This region appears structurally homologous to the first β-strand of the core fold found in the iron transporters FepA and FhuA.

ACKNOWLEDGMENT

We thank Christian Altenbach and Wayne Hubbell for providing copies of their LabView software for the analysis of EPR data and Kalman Hideg for providing the diamagnetic MTSL analogue.

REFERENCES

1. Moeck, G. S., and Coulton, J. W. (1998) *Mol. Microbiol. 28*, 675−681.
2. Klebba, P. E., and Newton, S. M. C. (1998) *Curr. Opin. Microbiol. 1*, 238−248.
3. Postle, K. (1999) *Nature Struct. Biol. 6*, 3−6.
4. Sansom, M. S. P. (1999) *Curr. Biol. 9*, R254−R257.
5. Killmann, H., Braun, M., Herrmann, C., and Braun, V. (2001) *J. Bacteriol. 183*, 3476−3487.
6. Ralf, K., Locher, K. P., and Van Gelder, P. (2000) *Mol. Microbiol. 37*, 239−253.
7. Buchanan, S. K., Smith, B. S., Venkatramanil, L., Xia, D., Esser, L., Palnitkar, M., Chakraborty, R., van der Helm, D., and Deisenhofer, J. (1999) *Nature Struct. Biol. 6*, 56−63.
8. Ferguson, A. D., Hofmann, E., Coulton, J. W., Diederichs, K., and Welte, W. (1998) *Science 282*, 2215−2220.
9. Locher, K. P., Rees, B., Koebnik, R., Mitschler, A., Moulinier, L., Rosenbusch, J. P., and Moras, D. (1998) *Cell 95*, 771−778.
10. Ferguson, A. D., Chakraborty, R., Smith, B. S., Esser, L., van der Helm, D., and Deisenhofer, J. (2002) *Science 295*, 1715−1719.
11. Gudmundsdottir, A., Bell, P. E., Lundrigan, M. D., Bradbeer, C., and Kadner, R. J. (1989) *J. Bacteriol. 171*, 6526−6533.
12. Merianos, H. J., Cadieux, N., Lin, C. H., Kadner, R., and Cafiso, D. S. (2000) *Nature Struct. Biol. 7*, 205−209.
13. Cadieux, N., and Kadner, R. J. (1999) *Proc. Natl. Acad. Sci. U.S.A. 96*, 10673−10678.
14. Cadieux, N., Bradbeer, C., and Kadner, R. (2000) *J. Bacteriol. 182*, 5954−5961.
15. Coggshall, K. A., Cadieux, N., Piedmont, C., Kadner, R., and Cafiso, D. S. (2001) *Biochemistry 40*, 13946−13971.
16. Usher, K. C., Ozkan, E., Gardner, K. H., and Deisenhofer, J. (2001) *Proc. Natl. Acad. Sci. U.S.A. 98*, 10676−10681.
17. Berliner, L. J., Grunwald, J., Hankovszky, H. O., and Hideg, K. (1982) *Anal. Biochem. 119*, 450−455.
18. Gross, A., Columbus, L., Hideg, K., Altenbach, C., and Hubbell, W. L. (1999) *Biochemistry 38*, 10324−10335.
19. Bassford, P. J. J., and Kadner, R. J. (1977) *J. Bacteriol. 132*, 796−805.
20. Fanucci, G. E., Cadieux, N., Piedmont, C. A., Kadner, R. J., and Cafiso, D. S. (2002) *Biochemistry 41*, 11543−11551.

21. Altenbach, C., Flitsch, S. L., Khorana, G., and Hubbell, W. L. (1989) *Biochemistry 28*, 7806−7812.
22. Farahbakhsh, Z. T., Altenbach, C., and Hubbell, W. L. (1992) *Photochem. Photobiol. 56*, 1019−1033.
23. Altenbach, C. A., Oh, K. J., Trabanino, R. J., Hideg, K., and Hubbell, W. L. (2001) *Biochemistry 40*, 15471−15482.
24. Mchaourab, H., Lietzow, M., Hideg, K., and Hubbell, W. (1996) *Biochemistry 35*, 7692−7704.
25. Hubbell, W. L., Cafiso, D. S., and Altenbach, C. A. (2000) *Nature Struct. Biol. 7*, 735−739.
26. Columbus, L., and Hubbell, W. L. (2002) *Trends Biochem. Sci. 27*, 288−295.
27. Columbus, L., Kalai, T., Jeko, J., Hideg, K., and Hubbell, W. L. (2001) *Biochemistry 40*, 3228−3846.
28. Kokorin, A. I., Zamaraev, K. I., Grigoryan, G. L., Ivanov, V. P., and Rosantzev, E. G. (1972) *Biofizika 17*, 34−41.
29. Hubbell, W. L., and Altenbach, C. (1994) *Curr. Opin. Struct. Biol. 4*, 566−573.
30. Oh, K. J., Zhan, H., Cui, C., Altenbach, C., Hubbell, W. L., and Collier, R. J. (1999) *Biochemistry 38*, 10336−10343.
31. Rabenstein, M. D., and Shin, Y. K. (1995) *Proc. Natl. Acad. Sci. U.S.A. 92*, 8239−8243.

BI027120Z